ACS Biomaterials SCIENCE & ENGINEERING

pubs.acs.org/journal/abseba

Article

Supramolecular Assembly of His-Tagged Fluorescent Protein Guests within Coiled-Coil Peptide Crystal Hosts: Three-Dimensional Ordering and Protein Thermal Stability

Ryan W. Curtis, Kevin T. Scrudders, James R. W. Ulcickas, Garth J. Simpson, Shalini T. Low-Nam, and Jean Chmielewski*

Cite This: https://doi.org/10.1021/acsbiomaterials.2c00155

Read Online

ACCESS | Metrics & More | Article Recommendations | Supporting Information

ABSTRACT: The use of biomaterials for the inclusion and stabilization of biopolymers is an ongoing challenge. Herein, we disclose three-dimensional (3D) coiled-coil peptide crystals with metal ions that include and overgrow His-tagged fluorescent proteins within the crystal. The protein guests are found within two symmetry-related growth sectors of the crystalline host that are associated with faces of the growing crystal that display ligands for metal ions. The fluorescent proteins are included within this "hourglass" region of the crystals at a notably high level, display order within the crystal hosts, and demonstrate sufficiently tight packing to enable energy transfer between a donor−acceptor pair. His-tagged fluorescent proteins display remarkable thermal stability to denaturation over extended periods of time (days) at high temperatures when within the crystals. Ultimately, this strategy may prove useful for the prolonged storage of thermally sensitive biopolymer guests within a 3D crystalline matrix.

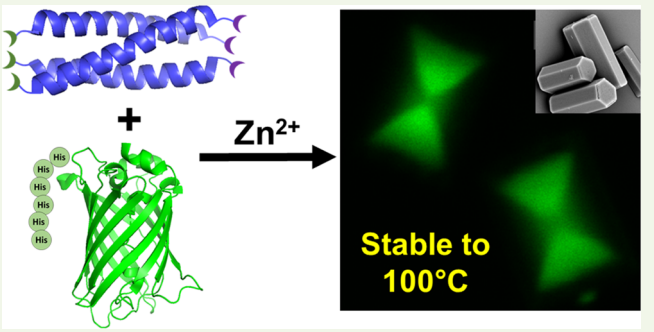

KEYWORDS: *coiled-coil, crystal, His-tagged protein, metal-dependent, thermal stability*

INTRODUCTION

Coiled-coil peptides have been used as building blocks to generate a variety of higher-order assemblies,[1] including fibers,[2−6] nanoblocks,[7] spherical cages,[8−12] nanotubes,[13] crystals,[14−16] hydrogels,[17−19] and three-dimensional (3D) matrices.[20] In some cases, these assemblies have been loaded with cargo, such as fluorophores,[2,14,20] dextrans,[13] peptides,[11] and proteins.[9,10] Incorporating cargoes with a diverse range of functionalities into such biomaterials with precise spatial control is an important challenge in biotechnology.[21] Proteins represent a particularly intriguing cargo as they perform a wide variety of functions,[22] but their complexity also makes their inclusion within biomaterials in a fully folded form a challenge.[23,24] Aggregation is a critical issue during the storage of proteins, and at elevated temperatures, protein unfolding followed by aggregation is a major mechanism for the loss of function.[25,26] Preserving the tertiary structure of proteins within biomaterials could facilitate the development of robust enzyme catalysts or eliminate the "cold-chain" storage and transport barriers in biopharmaceutical development. The isolation of proteins reversibly within crystalline biomaterials, for example, could be a powerful means to confront these challenges.

One method of ordering proteins has focused on incorporating His-tagged proteins onto two-dimensional (2D) arrays on Ni−nitrilotriacetic acid (NTA) surfaces for applications in high-throughput screening and cell culture.[27,28] There are also examples of proteins encapsulated within three-dimensional (3D) crystals,[29−39] and a limited number of these studies have addressed the thermal stability of the protein.[30,38] Kahr and co-workers, for instance, have investigated α-lactose crystals as a host for green fluorescent protein (GFP).[30,34] GFP was found localized to a specific growing face of the lactose crystals at modest encapsulation levels (1:10^6, GFP/lactose), with enhanced protein stability at elevated temperatures (60 °C for 1 h).[30] Protein crystals have also been used as hosts for other proteins. For instance, cross-linked 3D crystals of the *Campylobacter jejuni* (CJ) protein contain large pores that were used to encapsulate horseradish peroxidase (HRP). HRP displayed higher activity within the CJ crystals at an elevated temperature (45 °C) than at room temperature, presumably due to increased substrate penetration into the crystals.[38] In an effort to bridge these 2D and 3D experiments, herein, we

Received: February 8, 2022
Accepted: March 21, 2022

describe 3D crystals of a ligand-modified coiled-coil peptide and metal ions that serve as hosts for encapsulated His-tagged fluorescent protein guests. Proteins were found included with high loading levels in close proximity within the peptide/metal ion crystals in an ordered manner. The proteins were released through facile dissolution with chelators and displayed notable thermal stability.

RESULTS AND DISCUSSION

Metal-binding ligands within proteins and peptides have been used to promote assembly into highly ordered 3D crystalline materials, such as those formed from mutated cytochrome cb_{562},[40] T4 lysozyme,[41] ferritin,[42] nucleic acid-binding proteins,[43,44] and ligand-modified coiled coils with metal ions.[14−16] In this study, a trimeric coiled-coil peptide based on the GCN4 leucine zipper (GCN4-p2L) was used that contained ligands at the N-terminus (nitrilotriacetic acid—NTA) and C-terminus (di-histidine—His_2) for metal-promoted assembly (Figure 1a). GCN4-p2L has been reported to

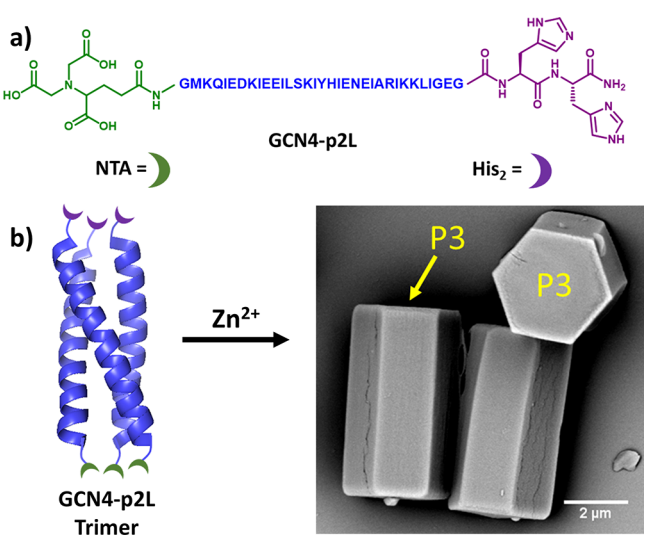

Figure 1. Schematic representation of the GCN4-p2L peptide and Zn(II)-mediated assembly. (a) Sequence of GCN4-p2L with metal-binding ligands. (b) Representation of the assembly of GCN4-p2L upon the addition of Zn(II) into hexagonal crystals shown with scanning electron microscopy (SEM). P3 crystal faces are highlighted.

assemble into hexagonal crystals upon the addition of divalent metal ions (Figure 1b), and X-ray analysis of the peptide crystals displayed hexagonal packing of the coiled-coil trimers with the ligands directed toward the growing P3 face (Figure 1b).[14] We sought to explore if ligands positioned on the P3 face of these growing crystals could be used to bring His-tagged protein cargo within the crystals in a metal-dependent fashion. As such, we used green fluorescent protein (GFP) as a model protein guest that may be incorporated and overgrown within these peptide crystals. The dramatic increase in the size of the potential cargo—from His-tagged fluorophore (fluorescein molecular weight (MW) 332) used in our previous studies[14] to a His-tagged protein (GFP MW 27 000)—would be a significant advancement if the latter was included within the crystals. Additionally, the fluorescence of GFP is dependent on proper folding,[45] and its β barrel is somewhat comparable in size to the trimeric coiled coil of GCN4-p2L, which may facilitate overgrowth within the peptide crystal.[46,47]

With these criteria in mind, we sought to incorporate enhanced green fluorescent protein (EGFP) with an N-terminal His_6-tag into the GCN4-p2L crystals during their growth. The peptide (1 mM) and $ZnCl_2$ (1 mM) were combined with EGFP (7.0 μM) in 3-(*N*-morpholino)-propanesulfonic acid (MOPS) buffer (20 mM, pH 7.1) (Figure 2a). A precipitate immediately formed that was collected after 1 h and washed. First, scanning electron microscopy (SEM) was used to monitor the overall morphology; crystals of ∼5 μm were obtained with a hexagonal prism shape, which were similar to those observed without EGFP (Figures 1b and S3). To determine if the folded EGFP was located within the coiled-coil peptide crystals, we employed confocal microscopy to achieve optical sectioning and diffraction-limited resolution of EGFP incorporation. The resultant crystal assemblies displayed a strong green fluorescence that was mostly confined to two symmetrical sections of the crystal in an "hourglass" orientation (Figure 2b). A low level of fluorescence was also observed outside of the hourglass regions, perhaps due to EGFP having some interactions with the coiled-coil peptides themselves.

Based on the crystal structure of the GCN4-p2L crystals, the ends of the hexagonal crystals (the P3 face—Figure 1b) would be decorated with the ligands from the termini of the GCN4-p2L coiled coils. This would be the surface upon which the His-tagged EGFP would bind to in a metal ion-dependent manner as the crystal grew.

The observed hourglass pattern would form, therefore, when the His-tag of EGFP bound to available metal-charged ligands on the two symmetry-related, growing P3 faces at the ends of the crystal. As those faces grow in area, so would the subvolume associated with EGFP fluorescence. We additionally evaluated the red fluorescent protein His-tagged mCherry (7.0 μM), and crystals with red fluorescence in an hourglass pattern were also obtained (Figure 2c,d). These data, in addition to the SEM, demonstrate that these protein guests do not preclude the formation of the hexagonal crystal morphology when incorporated within the crystals. Importantly, the observed fluorescence indicates that EGFP and mCherry were incorporated within the crystals in their properly folded forms, indicating that large guests, such as a protein, can bind to the P3 face and then be overgrown within the peptide crystals.

Determining the levels of protein guest incorporated into the GCN4-p2L/Zn^{2+} crystals was essential to properly evaluate their capabilities as vessels to hold proteins. A beneficial feature of these peptide crystals is that they undergo facile dissolution under mild conditions with chelators, so as to release and quantitate the encapsulated EGFP within the crystals. The crystals were treated with ethylenediaminetetraacetato (EDTA) (10 mM) for 10 min for dissolution, and the levels of peptide and protein were quantitated by ultraperformance liquid chromatography (UPLC) and fluorescence spectroscopy, respectively, using standard curves. Through this analysis, we found an ∼200:1 ratio of peptide to protein or one protein guest for every 60−70 coiled-coil units. Most of the fluorescence was localized to the hourglass region that accounts for ∼50% of the total volume of the crystal. Therefore, within the hourglass section of the crystal, there is 1 protein guest for every 30−35 coiled coils. This is a striking level of incorporation of the guest EGFP within the intact crystal host.

https://doi.org/10.1021/acsbiomaterials.2c00155
ACS Biomater. Sci. Eng. XXXX, XXX, XXX−XXX

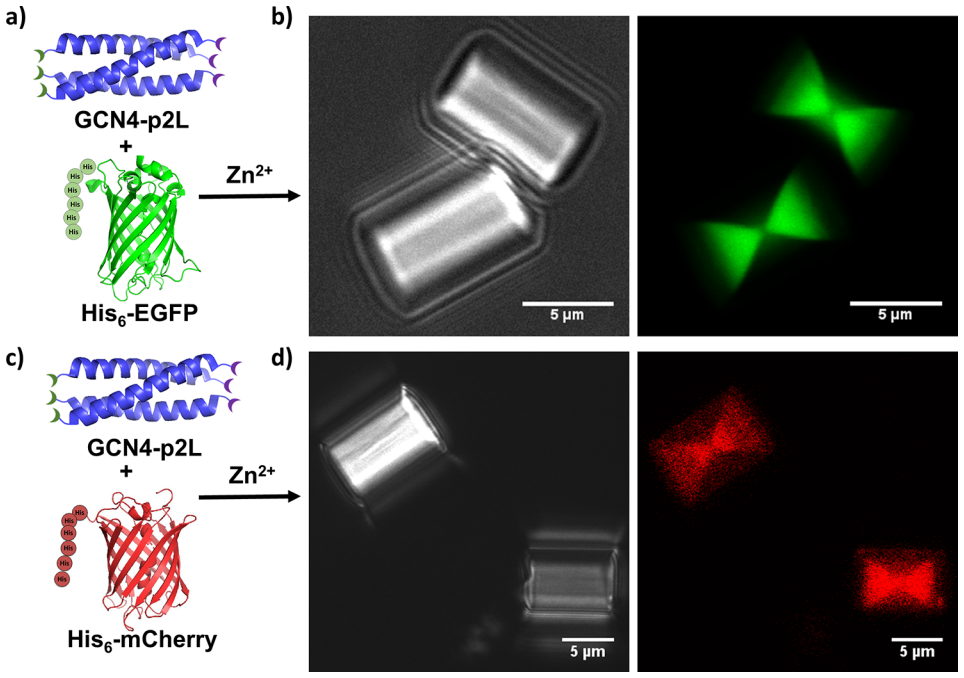

Figure 2. Incorporation of His-tagged proteins into hexagonal crystals. Schematic representation of the incorporation of (a) EGFP and (c) mCherry. Brightfield (left) and fluorescence (right) confocal images of crystals formed from GCN4-p2L (1 mM) incubated in 20 mM MOPS pH 7.1 with $ZnCl_2$ (1 mM) and (b) EGFP (7.0 μM) or (d) mCherry (7.0 μM).

With this high level of inclusion of the guest protein, it may be that the packing of coiled coils within the host crystal would be disrupted as compared to crystals without guests. We analyzed the crystals with small- and wide-angle X-ray scattering (SAXS/WAXS) to look at their internal packing. The SAXS/WAXS profiles of the crystals with and without EGFP were very similar, with signals at the same q values (Figure S5). These data indicate that the overall packing of the host crystals is maintained in the open-packed hexagonal arrangement and is not significantly altered by the inclusion of the EGFP protein guest. It may be that the guest proteins are not particularly ordered in terms of their distribution within the crystal, thus not providing much of a signal in the SAXS/WAXS experiment.

To study the protein organization within the crystals, we turned to fluorescence polarization imaging. If the chromophores of the fluorescent proteins are aligned in mostly one orientation, as opposed to a random distribution, emission anisotropy as a function of the angle of polarization would be expected.[30,48] When the GCN4-p2L crystals containing EGFP were interrogated with a two-photon emission fluorescence microscope with a rotating polarizer, the intensity of the fluorescence emission was found to fluctuate as a function of the angle of polarization (Figures 3 and S4). This indicates that there is a level of order with regard to the orientation of the EGFP molecules within the crystals. Taken together, these data suggest that the hexagonal arrangement of the coiled coils within the crystal was mostly maintained in the presence of a protein guest, with additional order in the alignment of EGFP proteins with respect to one another.

Simultaneous incorporation of EGFP and mCherry during GCN4-p2L crystallization provides information about the potential for concurrent protein delivery and proximities between adjacent FPs. We initially used mCherry and EGFP (7.0 μM of total protein) with a molar ratio of 5:1 of

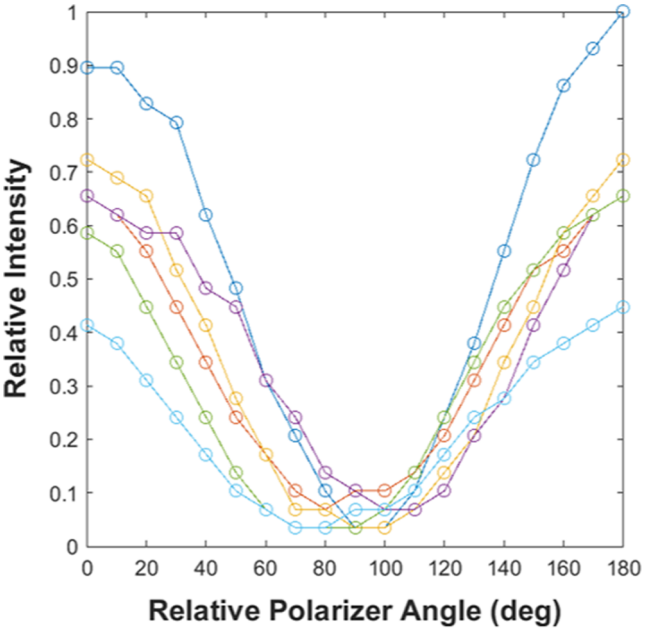

Figure 3. Intensity of a two-photon excitation (800 nm) fluorescence signal of various GCN4-p2L/EGFP crystals as a function of the angle of polarization of fluorescence emission. An angle of zero corresponds to the same angle as the incident laser polarization. Each set of values corresponds to a single crystal.

mCherry/EGFP since mCherry has a lower level of brightness. Both proteins were incorporated into single-crystal lattices and imaged by confocal microscopy (Figure 4a,b). Substantial overlay of green and red fluorescent signals demonstrated colocalization of the protein guests (Figure 4c). We concluded that some of the mCherry and EGFP are within diffraction-limited spacings of about 250 nm.

https://doi.org/10.1021/acsbiomaterials.2c00155
ACS Biomater. Sci. Eng. XXXX, XXX, XXX−XXX

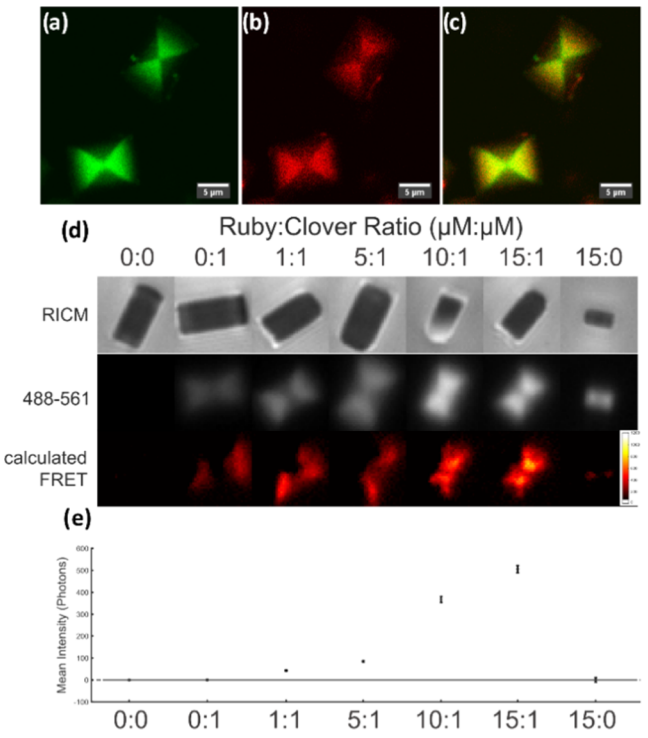

Figure 4. Simultaneous incorporation of two fluorescent proteins. (a) Green fluorescence, (b) red fluorescence, and (c) green and red overlay confocal images of crystals formed by GCN4-p2L (1 mM) with EGFP (1.4 μM) and mCherry (5.6 μM) and $ZnCl_2$ (1 mM) in MOPS buffer (20 mM, pH 7.1). (d) Reflection interference contrast microscopy (RICM), Förster resonance energy transfer (FRET) channel, and calculated FRET channel images of crystals formed by GCN4-p2L (1 mM) with given concentrations of mClover3 and mRuby3 in $ZnCl_2$ (1 mM) in MOPS buffer (20 mM, pH 7.1). (e) Calculated Förster resonance energy-transfer (FRET) sensitized emission of populations of crystals with the designated ratio of mRuby3/mClover3. Error bars are from the standard error of the mean.

Based on the measured peptide-to-protein ratio of ~35:1 within the hourglass segments of the crystals, we predicted that two spectrally distinct fluorescent proteins could be in a close enough proximity to enable Förster resonance energy transfer (FRET). We incorporated the FRET pair mClover3 and mRuby3, each with an N-terminal His-tag, into GCN4-p2L crystals over a range of ratios, and either alone or together the same hourglass fluorescence was observed with colocalization (Figures 4b,c and S6–S8). These fluorescent proteins have enhanced brightness and have a Förster radius on the order of just over 6 nm.[49] To probe the interprotein distances within the crystal by FRET, therefore, the donor, mClover3, ratio within the crystals was fixed and the acceptor, mRuby3, was doped up to a 1:15 molar ratio, respectively. The resulting crystals were imaged in an epifluorescence configuration (Figure 4d). As the incorporation of the acceptor mRuby3 protein was increased, a definitive sensitized mRuby3 emission was measured. These data indicate a close packing of the guest proteins within the hexagonally packed GCN4-p2L crystalline host (Figure 4d,e).

Based on the X-ray crystal structure of the GCN4-p2L peptide crystals and the data for His-tagged fluorescent protein inclusion above, we have modeled how the guest protein may be incorporated into the host crystal lattice. The honeycomb hexagonal packing of the coiled-coil trimers within the crystal produces a central cavity that is too small (~3 nm) for protein binding (Figure 5b). The growing P3 face of the crystal would

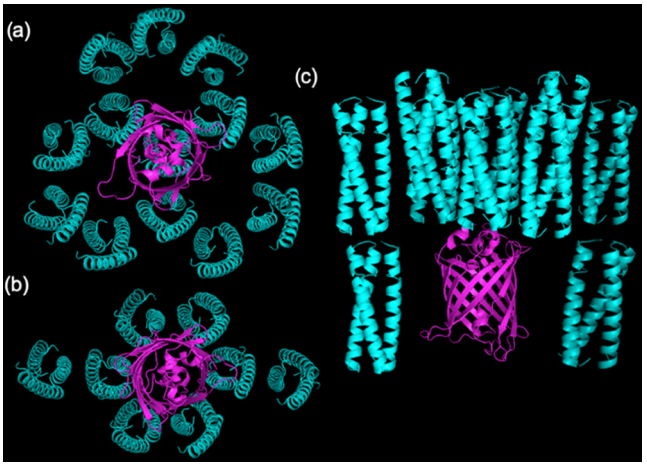

Figure 5. Depiction of the hexagonal honeycomb packing of GCN4-p2L from the X-ray structure of the crystals[14] (cyan) with models of GFP (purple) (a) positioned at the end of a coiled coil and (b) over the hexagonal channel and (c) demonstrating overgrowth of the coiled coils upon GFP inclusion (note: ligands and metals were not included for clarity).

display the ligands at the termini of the coiled coils. In the presence of metal ions, the His-tag of the fluorescent protein could bind to this face at a number of positions (Figure 5a,b) and then be grown over with additional trimeric coiled coils in a metal-dependent manner (Figure 5c). We know that the chromophores with the FPs are aligned within the crystals from the polarized fluorescence experiments, so the directionality of the protein with respect to the P3 face is mostly maintained throughout the crystal. Since we only observed a signal in the SAXS/WAXS data corresponding to the coiled-coil packing within the crystal, it may be that the distribution of a protein guest within the crystal lattice is not significantly ordered.

As described above, the GCN4-p2L peptide crystals displayed metal-binding ligands on the P3 face.[14] We additionally sought to harness these free ligands to attach His-tagged proteins to the surface of the fully formed crystals in a metal ion-dependent fashion. Thus, pre-formed crystals (1 mM GCN4-p2L/1 mM $ZnCl_2$) were treated with $NiCl_2$ (1 mM) for 1 h and washed. These Ni(II)-treated crystals were then incubated with either His-tagged EGFP or mCherry (7.0 μM). When visualized via confocal microscopy, fluorescence attributed to the proteins was observed on both of the crystal's P3 faces, as well as on the other sides of the crystals (Figure 6a,b). These data suggest that there are nonmetal-mediated interactions involved in protein–crystal binding. To test if metal ions are required for protein binding to the crystal surface, we incubated pre-formed crystals with His-tagged EGFP (7.0 μM) without pretreatment with Ni(II) ions. The resultant assemblies also fluoresced green on all sides (Figure S10); however, the level of fluorescence was noticeably lower without Ni(II) treatment. These data show that Ni(II) is not necessary for protein interactions with pre-formed crystals, but the addition of metal ions does maximize protein levels on the crystal surface. Similar data were observed with $ZnCl_2$ pretreatment as well (data not shown).

https://doi.org/10.1021/acsbiomaterials.2c00155
ACS Biomater. Sci. Eng. XXXX, XXX, XXX–XXX

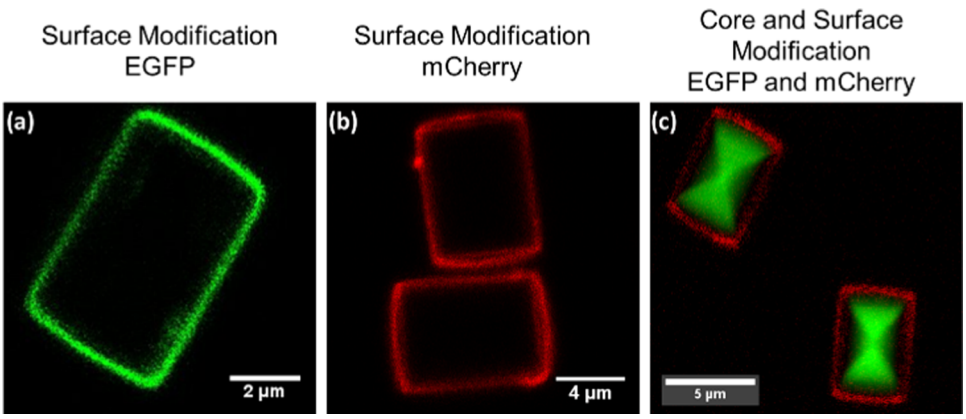

Figure 6. Fluorescence confocal images of GCN4-p2L crystals treated with $NiCl_2$ for 1 h followed by treatment with (a) EGFP (7.0 μM) or (b) mCherry (7.0 μM) for 12 h. (c) Fluorescence overlay confocal image of GCN4-p2L/EGFP crystals treated with $NiCl_2$ for 1 h followed by mCherry for 12 h.

Additionally, we sought to add two different proteins to the peptide crystals in two distinct regions within and on the surface of the crystal. Therefore, crystals that were formed in the presence of His-tagged EGFP were subsequently incubated with $NiCl_2$, followed by His-tagged mCherry. Confocal microscopy of the resulting crystals showed a green fluorescent hourglass pattern within the crystals as observed above with EGFP but now with noticeable red fluorescence on the crystal surface from mCherry (Figure 6c).

Proteins isolated within the crystalline peptide matrix may be less prone to thermally induced unfolding and aggregation. To test the hypothesis that the crystals could serve as protein stabilization vehicles, samples of GCN4-p2L crystals with EGFP (1 mM GCN4-p2L/7.0 μM His-tagged EGFP) were heated over different time periods. Because denaturation of EGFP causes the protein to lose its fluorescence, the amount of protein that remains folded was measured by levels of fluorescence. Remarkably, the crystals remained highly fluorescent even after they were heated to 100 °C for 1 h (Figure 7a). In comparison, a solution of EGFP in phosphate-buffered saline (PBS) lost all fluorescence after incubation at 100 °C for 1 min (Figure S11). Because of their size (~5 μm in length) and the lack of crystal aggregation, flow cytometry was used to monitor the fluorescence of populations of crystals.[50,51] Crystals containing His-tagged EGFP maintained 93% of their initial fluorescence after being incubated at 70 °C for 4 days, and after 1 week, 70% of the fluorescence was retained. In contrast, a solution of His-tagged EGFP in PBS lost all fluorescence after incubation at 70 °C for 1 day (Figure 7b).

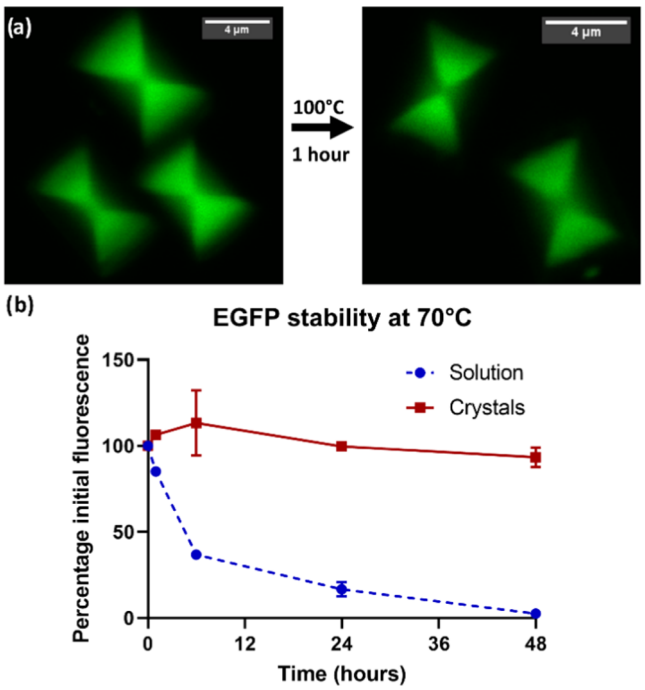

Figure 7. Stability of EGFP within the crystals. (a) Fluorescence confocal images of crystals before and after incubation at 100 °C for 1 h using the same laser intensity. (b) Percentage of fluorescence retained by EGFP retained in crystals or in solution upon incubation at 70 °C over time.

CONCLUSIONS

In conclusion, we have demonstrated the ability to incorporate and overgrow His-tagged fluorescent proteins within the 3D matrix of growing coiled-coil peptide crystals with high levels of efficiency. Fluorescence polarization experiments confirm that there is ordering of the protein guests within the crystalline host, and SAXS/WAXS data confirm that the overall packing of the peptide within the crystals has been preserved. Experiments with a FRET pair of fluorescent proteins, mClover3 and mRuby3, indicate that protein guests may be packed in very close proximities, as close as 6 nm.[49] Furthermore, we established that EGFP guests are notably more stable to extreme temperatures over extended time periods when isolated within the crystals as compared to those in solution. This ability to include folded protein guests within crystalline hosts could have far-ranging applications from room-temperature storage of biopharmaceuticals to protein arrays for structural elucidation.

ASSOCIATED CONTENT

Supporting Information

The Supporting Information is available free of charge at https://pubs.acs.org/doi/10.1021/acsbiomaterials.2c00155.

Methods; HPLC purity chromatogram; MALDI mass spectrum; SEM image; confocal images of crystals; FRET; addition of His-tagged proteins to the surface of crystals formed; and picture of EGFP in 1× PBS (PDF)

https://doi.org/10.1021/acsbiomaterials.2c00155
ACS Biomater. Sci. Eng. XXXX, XXX, XXX−XXX

AUTHOR INFORMATION

Corresponding Author

Jean Chmielewski − *Department of Chemistry, Purdue University, West Lafayette, Indiana 47907-2084, United States;* orcid.org/0000-0003-4958-7175; Email: chml@purdue.edu

Authors

Ryan W. Curtis − *Department of Chemistry, Purdue University, West Lafayette, Indiana 47907-2084, United States*

Kevin T. Scrudders − *Department of Chemistry, Purdue University, West Lafayette, Indiana 47907-2084, United States;* orcid.org/0000-0001-5309-7967

James R. W. Ulcickas − *Department of Chemistry, Purdue University, West Lafayette, Indiana 47907-2084, United States*

Garth J. Simpson − *Department of Chemistry, Purdue University, West Lafayette, Indiana 47907-2084, United States;* orcid.org/0000-0002-3932-848X

Shalini T. Low-Nam − *Department of Chemistry, Purdue University, West Lafayette, Indiana 47907-2084, United States;* orcid.org/0000-0001-7055-9369

Complete contact information is available at: https://pubs.acs.org/10.1021/acsbiomaterials.2c00155

Author Contributions

The manuscript was written through contributions of all authors. All authors have given approval to the final version of the manuscript.

Notes

The authors declare no competing financial interest.

ACKNOWLEDGMENTS

The authors are grateful to the National Science Foundation (CHE-2108722) for support of this work.

REFERENCES

(1) Robson Marsden, H.; Kros, A. Self-Assembly of Coiled Coils in Synthetic Biology: Inspiration and Progress. *Angew. Chem., Int. Ed.* **2010**, *49*, 2988−3005.

(2) Gunasekar, S. K.; Anjia, L.; Matsui, H.; Montclare, J. K. Effects of Divalent Metals on Nanoscopic Fiber Formation and Small Molecule Recognition of Helical Proteins. *Adv. Funct. Mater.* **2012**, *22*, 2154−2159.

(3) Xu, C.; Liu, R.; Mehta, A. K.; Guerrero-Ferreira, R. C.; Wright, E. R.; Dunin-Horkawicz, S.; Morris, K.; Serpell, L. C.; Zuo, X.; Wall, J. S.; Conticello, V. P. Rational Design of Helical Nanotubes from Self-Assembly of Coiled-Coil Lock Washers. *J. Am. Chem. Soc.* **2013**, *135*, 15565−15578.

(4) Burgess, N. C.; Sharp, T. H.; Thomas, F.; Wood, C. W.; Thomson, A. R.; Zaccai, N. R.; Brady, R. L.; Serpell, L. C.; Woolfson, D. N. Modular Design of Self-Assembling Peptide-Based Nanotubes. *J. Am. Chem. Soc.* **2015**, *137*, 10554−10562.

(5) Thomas, F.; Burgess, N. C.; Thomson, A. R.; Woolfson, D. N. Controlling the Assembly of Coiled-Coil Peptide Nanotubes. *Angew. Chem., Int. Ed.* **2016**, *55*, 987−991.

(6) Tian, Y.; Polzer, F. B.; Zhang, H. V.; Kiick, K. L.; Saven, J. G.; Pochan, D. J. Nanotubes, Plates, and Needles: Pathway-Dependent Self-Assembly of Computationally Designed Peptides. *Biomacromolecules* **2018**, *19*, 4286−4298.

(7) Nambiar, M.; Wang, L.-S.; Rotello, V.; Chmielewski, J. Reversible Hierarchical Assembly of Trimeric Coiled-Coil Peptides into Banded Nano- and Microstructures. *J. Am. Chem. Soc.* **2018**, *140*, 13028−13033.

(8) Fletcher, J. M.; Harniman, R. L.; Barnes, F. R. H.; Boyle, A. L.; Collins, A.; Mantell, J.; Sharp, T. H.; Antognozzi, M.; Booth, P. J.; Linden, N.; Miles, M. J.; Sessions, R. B.; Verkade, P.; Woolfson, D. N. Self-Assembling Cages from Coiled-Coil Peptide Modules. *Science* **2013**, *340*, 595−599.

(9) Ross, J. F.; Bridges, A.; Fletcher, J. M.; Shoemark, D.; Alibhai, D.; Bray, H. E. V.; Beesley, J. L.; Dawson, W. M.; Hodgson, L. R.; Mantell, J.; Verkade, P.; Edge, C. M.; Sessions, R. B.; Tew, D.; Woolfson, D. N. Decorating Self-Assembled Peptide Cages with Proteins. *ACS Nano* **2017**, *11*, 7901−7914.

(10) Beesley, J. L.; Baum, H. E.; Hodgson, L. R.; Verkade, P.; Banting, G. S.; Woolfson, D. N. Modifying Self-Assembled Peptide Cages To Control Internalization into Mammalian Cells. *Nano Lett.* **2018**, *18*, 5933−5937.

(11) Morris, C.; Glennie, S. J.; Lam, H. S.; Baum, H. E.; Kandage, D.; Williams, N. A.; Morgan, D. J.; Woolfson, D. N.; Davidson, A. D. A Modular Vaccine Platform Combining Self-Assembled Peptide Cages and Immunogenic Peptides. *Adv. Funct. Mater.* **2019**, *29*, No. 1807357.

(12) Galloway, J. M.; Bray, H. E. V.; Shoemark, D. K.; Hodgson, L. R.; Coombs, J.; Mantell, J. M.; Rose, R. S.; Ross, J. F.; Morris, C.; Harniman, R. L.; Wood, C. W.; Arthur, C.; Verkade, P.; Woolfson, D. N. De Novo Designed Peptide and Protein Hairpins Self-Assemble into Sheets and Nanoparticles. *Small* **2021**, *17*, No. 2100472.

(13) Nambiar, M.; Nepal, M.; Chmielewski, J. Self-Assembling Coiled-Coil Peptide Nanotubes with Biomolecular Cargo Encapsulation. *ACS Biomater. Sci. Eng.* **2019**, *5*, 5082−5087.

(14) Nepal, M.; Sheedlo, M. J.; Das, C.; Chmielewski, J. Accessing Three-Dimensional Crystals with Incorporated Guests through Metal-Directed Coiled-Coil Peptide Assembly. *J. Am. Chem. Soc.* **2016**, *138*, 11051−11057.

(15) Tavenor, N. A.; Murnin, M. J.; Horne, W. S. Supramolecular Metal-Coordination Polymers, Nets, and Frameworks from Synthetic Coiled-Coil Peptides. *J. Am. Chem. Soc.* **2017**, *139*, 2212−2215.

(16) Scheib, K. A.; Tavenor, N. A.; Lawless, M. J.; Saxena, S.; Horne, W. S. Understanding and Controlling the Metal-Directed Assembly of Terpyridine-Functionalized Coiled-Coil Peptides. *Chem. Commun.* **2019**, *55*, 7752−7755.

(17) Dexter, A. F.; Fletcher, N. L.; Creasey, R. G.; Filardo, F.; Boehm, M. W.; Jack, K. S. Fabrication and Characterization of Hydrogels Formed from Designer Coiled-Coil Fibril-Forming Peptides. *RSC Adv.* **2017**, *7*, 27260−27271.

(18) Tunn, I.; Harrington, M. J.; Blank, K. G. Bioinspired Histidine−Zn2+ Coordination for Tuning the Mechanical Properties of Self-Healing Coiled Coil Cross-Linked Hydrogels. *Biomimetics* **2019**, *4*, No. 25.

(19) Meleties, M.; Katyal, P.; Lin, B.; Britton, D.; Montclare, J. K. Self-Assembly of Stimuli-Responsive Coiled-Coil Fibrous Hydrogels. *Soft Matter* **2021**, *17*, 6470−6476.

(20) Jorgensen, M. D.; Chmielewski, J. Reversible Crosslinked Assembly of a Trimeric Coiled-coil Peptide into a Three-dimensional Matrix for Cell Encapsulation and Release. *J. Pept. Sci.* **2022**, *28*, No. e3302.

(21) Tibbitt, M. W.; Rodell, C. B.; Burdick, J. A.; Anseth, K. S. Progress in Material Design for Biomedical Applications. *Proc. Natl. Acad. Sci. U.S.A.* **2015**, *112*, 14444−14451.

(22) Krishna, O. D.; Kiick, K. L. Protein- and Peptide-Modified Synthetic Polymeric Biomaterials. *Biopolymers* **2010**, *94*, 32−48.

(23) Spicer, C. D.; Pashuck, E. T.; Stevens, M. M. Achieving Controlled Biomolecule−Biomaterial Conjugation. *Chem. Rev.* **2018**, *118*, 7702−7743.

(24) Clegg, J. R.; Peppas, N. A. Molecular Recognition with Soft Biomaterials. *Soft Matter* **2020**, *16*, 856−869.

(25) Fields, G. B.; Alonso, D. O. V.; Stigter, D.; Dill, K. A. Theory for the Aggregation of Proteins and Copolymers. *J. Phys. Chem. A* **1992**, *96*, 3974−3981.

(26) Dobson, C. M. Protein Folding and Misfolding. *Nature* **2003**, *426*, 884−890.

(27) Thompson, D. H.; Zhou, M.; Grey, J.; Kim, H. Design, Synthesis, and Performance of NTA-Modified Lipids as Templates for Histidine-Tagged Protein Crystallization. *Chem. Lett.* **2007**, *36*, 956−975.
(28) Wasserberg, D.; Cabanas-Danés, J.; Prangsma, J.; O'Mahony, S.; Cazade, P.-A.; Tromp, E.; Blum, C.; Thompson, D.; Huskens, J.; Subramaniam, V.; Jonkheijm, P. Controlling Protein Surface Orientation by Strategic Placement of Oligo-Histidine Tags. *ACS Nano* **2017**, *11*, 9068−9083.
(29) Chmielewski, J.; Lewis, J. J.; Lovell, S.; Zutshi, R.; Savickas, P.; Mitchell, C. A.; Subramony, J. A.; Kahr, B. Single-Crystal Matrix Isolation of Biopolymers. *J. Am. Chem. Soc.* **1997**, *119*, 10565−10566.
(30) Kurimoto, M.; Subramony, P.; Gurney, R. W.; Lovell, S.; Chmielewski, J.; Kahr, B. Kinetic Stabilization of Biopolymers in Single-Crystal Hosts: Green Fluorescent Protein in α-Lactose Monohydrate. *J. Am. Chem. Soc.* **1999**, *121*, 6952−6953.
(31) Wang, H. C.; Kurimoto, M.; Kahr, B.; Chmielewski, J. α-Lactose Monohydrate Single Crystals as Hosts for Matrix Isolation of Guest Biopolymers. *Bioorg. Med. Chem.* **2001**, *9*, 2279−2283.
(32) Geng, C.; Paukstelis, P. J. DNA Crystals as Vehicles for Biocatalysis. *J. Am. Chem. Soc.* **2014**, *136*, 7817−7820.
(33) Abe, S.; Ijiri, H.; Negishi, H.; Yamanaka, H.; Sasaki, K.; Hirata, K.; Mori, H.; Ueno, T. Design of Enzyme-Encapsulated Protein Containers by In Vivo Crystal Engineering. *Adv. Mater.* **2015**, *27*, 7951−7956.
(34) Shtukenberg, A. G.; Tripathi, K.; Ketchum, R.; Jeon, J. J.; Sanda, A.; Kahr, B. Incorporation of Macromolecules into α-Lactose Monohydrate Crystals. *Cryst. Growth Des.* **2016**, *16*, 4589−4598.
(35) Huber, T. R.; Hartje, L. F.; McPherson, E. C.; Kowalski, A. E.; Snow, C. D. Programmed Assembly of Host-Guest Protein Crystals. *Small* **2017**, *13*, No. 1602703.
(36) Ernst, P.; Plückthun, A.; Mittl, P. R. E. Structural Analysis of Biological Targets by Host:Guest Crystal Lattice Engineering. *Sci. Rep.* **2019**, *9*, No. 15199.
(37) Hashimoto, T.; Ye, Y.; Ui, M.; Ogawa, T.; Matsui, T.; Tanaka, Y. Protein Encapsulation in the Hollow Space of Hemocyanin Crystals Containing a Covalently Conjugated Ligand. *Biochem. Biophys. Res. Commun.* **2019**, *514*, 31−36.
(38) Kowalski, A. E.; Johnson, L. B.; Dierl, H. K.; Park, S.; Huber, T. R.; Snow, C. D. Porous Protein Crystals as Scaffolds for Enzyme Immobilization. *Biomater. Sci.* **2019**, *7*, 1898−1904.
(39) Li, Z.; Liu, L.; Zheng, M.; Zhao, J.; Seeman, N. C.; Mao, C. Making Engineered 3D DNA Crystals Robust. *J. Am. Chem. Soc.* **2019**, *141*, 15850−15855.
(40) Golub, E.; Subramanian, R. H.; Esselborn, J.; Alberstein, R. G.; Bailey, J. B.; Chiong, J. A.; Yan, X.; Booth, T.; Baker, T. S.; Tezcan, F. A. Constructing Protein Polyhedra via Orthogonal Chemical Interactions. *Nature* **2020**, *578*, 172−176.
(41) Laganowsky, A.; Zhao, M.; Soriaga, A. B.; Sawaya, M. R.; Cascio, D.; Yeates, T. O. An Approach to Crystallizing Proteins by Metal-Mediated Synthetic Symmetrization: Crystallization of Proteins by Metal-Mediated Symmetrization. *Protein Sci.* **2011**, *20*, 1876−1890.
(42) Bailey, J. B.; Tezcan, F. A. Tunable and Cooperative Thermomechanical Properties of Protein−Metal−Organic Frameworks. *J. Am. Chem. Soc.* **2020**, *142*, 17265−17270.
(43) Chen, H.; Zhou, K.; Wang, Y.; Zang, J.; Zhao, G. Self-Assembly of Engineered Protein Nanocages into Reversible Ordered 3D Superlattices Mediated by Zinc Ions. *Chem. Commun.* **2019**, *55*, 11299−11302.
(44) Malay, A. D.; Miyazaki, N.; Biela, A.; Chakraborti, S.; Majsterkiewicz, K.; Stupka, I.; Kaplan, C. S.; Kowalczyk, A.; Piette, B. M. A. G.; Hochberg, G. K. A.; Wu, D.; Wrobel, T. P.; Fineberg, A.; Kushwah, M. S.; Kelemen, M.; Vavpetič, P.; Pelicon, P.; Kukura, P.; Benesch, J. L. P.; Iwasaki, K.; Heddle, J. G. An Ultra-Stable Gold-Coordinated Protein Cage Displaying Reversible Assembly. *Nature* **2019**, *569*, 438−442.
(45) Bokman, S. H.; Ward, W. W. Renaturation of Aequorea Green-Fluorescent Protein. *Biochem. Biophys. Res. Commun.* **1981**, *101*, 1372−1380.
(46) Harbury, P. B.; Kim, P. S.; Alber, T. Crystal Structure of an Isoleucine-Zipper Trimer. *Nature* **1994**, *371*, 80−83.
(47) Orm, M.; Cubitt, A. B.; Kallio, K.; Gross, L. A.; Tsien, R. Y.; Remington, S. J. Crystal Structure of the Aequorea Victoria Green Fluorescent Protein. *Science* **1996**, *273*, 1392−1395.
(48) Inoué, S.; Shimomura, O.; Goda, M.; Shribak, M.; Tran, P. T. Fluorescence Polarization of Green Fluorescence Protein. *Proc. Natl. Acad. Sci. U.S.A.* **2002**, *99*, 4272−4277.
(49) Bajar, B. T.; Wang, E. S.; Lam, A. J.; Kim, B. B.; Jacobs, C. L.; Howe, E. S.; Davidson, M. W.; Lin, M. Z.; Chu, J. Improving Brightness and Photostability of Green and Red Fluorescent Proteins for Live Cell Imaging and FRET Reporting. *Sci. Rep.* **2016**, *6*, No. 20889.
(50) Pires, M. M.; Ernenwein, D.; Chmielewski, J. Selective Decoration and Release of His-Tagged Proteins from Metal-Assembled Collagen Peptide Microflorettes. *Biomacromolecules* **2011**, *12*, 2429−2433.
(51) Orozco, A. F.; Lewis, D. E. Flow Cytometric Analysis of Circulating Microparticles in Plasma. *Cytometry* **2010**, *77A*, 502−514.

https://doi.org/10.1021/acsbiomaterials.2c00155
ACS Biomater. Sci. Eng. XXXX, XXX, XXX−XXX